Modern Valence-Bond Description of Chemical Reaction Mechanisms: Diels−Alder Reaction

Peter B. Karadakov,[†] David L. Cooper,[‡] and Joseph Gerratt[§,⊥]

Contribution from the Department of Chemistry, University of Surrey, Guildford GU2 5XH, U.K., Department of Chemistry, University of Liverpool, P.O. Box 147, Liverpool L69 7ZD, U.K., and School of Chemistry, University of Bristol, Cantock's Close, Bristol BS8 1TS, U.K.

Received December 9, 1997. Revised Manuscript Received February 23, 1998

Abstract: The electronic mechanism for the gas-phase Diels−Alder cycloaddition reaction is studied through a combination of modern valence-bond (VB) theory in its spin-coupled (SC) form and intrinsic reaction coordinate calculations utilizing a complete-active-space self-consistent field (CASSCF) wave function. Throughout the reaction, the nonorthogonal SC orbitals resemble well-localized sp^x hybrids, each of which remains permanently attached to a single carbon atom. The changes in the shapes of these SC orbitals, together with the variations of the overlaps between neighboring orbitals, produce a lucid picture of the parallel breaking of the butadiene and ethene π bonds and of the formation of the two new σ bonds, closing the ring, and of the cyclohexene π bond. The analogue of classical VB resonance, namely, the active-space spin-coupling pattern within the SC wave function, shows no resonance well before and well after the transition structure (TS). At and around the TS, this pattern is dominated by two Kekulé Rumer spin functions of comparable weight. This and other resemblances to the well-known SC description of benzene (similar orbital shapes, equalization of the overlaps between neighboring orbitals) indicate clearly that the Diels−Alder reaction passes through a geometry, very close to the TS, at which it is aromatic. The visual changes in the SC wave function as the system follows the reaction path strongly suggest that the best schematic representation of the Diels−Alder reaction is through a "homolytic" mechanism, in which six half-arrows indicate the simultaneous breaking of the three π bonds on the reactants and formation of the three new bonds, two σ and one π, in the product.

Introduction

A satisfactory theoretical model of a chemical reaction mechanism should be able to answer two fundamental questions: Firstly, how do the energy and geometry of the ensemble of interacting atoms vary on the way from reactants to products, and secondly, what are the related changes in the electronic structure of the system. Quantum chemistry is becoming increasingly adept at providing an accurate answer to the first of these questions for an ever-widening range of chemical reactions. Large *ab initio* codes such as GAUSSIAN94[1] and GAMESS (U.S. version)[2] incorporate efficient optimization algorithms which can find equilibrium geometries, locate transition structures, and follow reaction paths using highly correlated wave functions. However, in parallel with the growing complexity of the wave function, the often radical changes in the electronic structure of a reacting system become more and more difficult to follow, visualize, and interpret. The renewal of interest in valence bond theory in recent years[3−8] serves to illustrate that chemists are no longer satisfied with accurate numbers only: There is a recognized need for qualitative models stemming from quantitative wave functions and highlighting general features and tendencies in chemical structure and reactivity. This is something which very few of the state-of-the-art quantum-chemical approaches can provide in a straightforward way, if at all.

Spin-coupled (SC) theory (for a recent review, see ref 9) is one of the most useful modern renditions of valence-bond (VB) ideas. The potential of this approach is well illustrated by the highly unorthodox (from the viewpoint of conventional molecular orbital theory) description which it provides for the π electron system of benzene.[10−12] The six π electrons populate a single product of six nonorthogonal orbitals, the spins of which are coupled in all five possible ways to achieve an overall singlet. The optimal orbitals turn out to be well-localized,

[†] University of Surrey.
[‡] University of Liverpool.
[§] University of Bristol.
[⊥] Deceased Oct 16, 1997.

(1) Frisch, M. J.; Trucks, G. W.; Schlegel, H. B.; Gill, P. M. W.; Johnson, B. G.; Robb, M. A.; Cheeseman, J. R.; Keith, T.; Petersson, G. A.; Montgomery, J. A.; Raghavachari, K.; Al-Laham, M. A.; Zakrzewski, V. G.; Ortiz, J. V.; Foresman, J. B.; Cioslowski, J.; Stefanov, B. B.; Nanayakkara, A.; Challacombe, M.; Peng, C. Y.; Ayala, P. Y.; Chen, W.; Wong, M. W.; Andres, J. L.; Replogle, E. S.; Gomperts, R.; Martin, R. L.; Fox, D. J.; Binkley, J. S.; Defrees, D. J.; Baker, J.; Stewart, J. P.; Head-Gordon, M.; Gonzalez, C.; Pople, J. A. *Gaussian 94, Revision D.4*; Gaussian, Inc.: Pittsburgh, PA, 1995.

(2) Schmidt, M. W.; Baldridge, K. K.; Boatz, J. A.; Elbert, S. T.; Gordon, M. S.; Jensen, J. H.; Koseki, S.; Matsunaga, N.; Nguyen, K. A.; Su, S. J.; Windus, T. L.; Dupuis, M.; Montgomery, J. A. *J. Comput. Chem.*; **1993**, *14*, 1347.

(3) Li, J. B. *Theor. Chim. Acta* **1996**, *110*, 35.

(4) Shaik, S.; Hiberty, P. C. *Adv. Quantum Chem.* **1995**, *26*, 99.

(5) Malcolm, N. O. J.; McDouall, J. J. W. *J. Comput. Chem.* **1994**, *15*, 1357.

(6) Hiberty, P. C.; Humbel, S.; Byrman, C. P.; Van Lenthe, J. H. *J. Chem. Phys.* **1994**, *101*, 5969.

(7) Bernardi, F.; Olivucci, M.; Robb, M. A. *J. Am. Chem. Soc.* **1992**, *114*, 1606.

(8) McWeeny, R. *Int. J. Quantum Chem.* **1990**, *S24*, 733.

(9) Gerratt, J.; Cooper, D. L.; Karadakov, P. B.; Raimondi, M. *Chem. Soc. Rev.* **1997**, *26*, 87.

(10) Cooper, D. L.; Gerratt, J.; Raimondi, M. *Nature* **1986**, *323*, 699.

(11) Gerratt, J. *Chem. Br.* **1987**, *23*, 327.

(12) Cooper, D. L.; Wright, S. C.; Gerratt, J.; Hyams, P. A.; Raimondi, M. *J. Chem. Soc., Perkin Trans. 2* **1989**, 719.

S0002-7863(97)04174-7 CCC: $15.00
Published on Web 04/14/1998

similar in shape to C($2p_\pi$) atomic orbitals with small symmetrical bulges toward neighboring carbons, while the optimal spin-coupling pattern is dominated by two equivalent Kekulé structures and has much smaller contributions from three equivalent Dewar (or para-bonded) structures. This picture bears striking resemblance to the classical VB description of benzene in terms of resonance structures taken from an organic chemistry textbook (one should now look in a rather old edition!), and yet it comes from a wave function of an adequate quality which accounts for most of the correlation energy incorporated in a "6 in 6" π space complete-active-space self-consistent field (CASSCF) calculation. The unique integration of chemical intuition and quantitative character within the SC descriptions of benzene and other aromatic[13−16] and antiaromatic[17,18] molecules suggests that the SC approach represents a very appropriate tool for theoretical studies of the mechanisms of reactions which are considered to pass through aromatic or to avoid antiaromatic transition structures.

In this paper we present the spin-coupled model for the evolution of the electronic structure of the reacting system during the course of a pericyclic reaction that has been the focus of numerous theoretical studies: the gas-phase Diels−Alder cycloaddition between *cis*-butadiene and ethene. The details of the mechanism for this reaction have been the subject of a prolonged argument between theoretical chemists using semiempirical and *ab initio* approaches.[19] Experimental evidence indicates that the concerted pathway is 2−7 kcal mol^{-1} below the stepwise alternative. On the whole, semiempirical studies tend to favor the stepwise mechanism while *ab initio* calculations give preference to the concerted path, although there are notable exceptions: For example, Houk et al.[20,21] found that within the "six electrons in six orbitals" CASSCF framework [CASSCF-(6,6)/6-31G*, geometries optimized at the same level of theory], the diradical intermediate from the stepwise pathway is 3.1 kcal mol^{-1} below the concerted transition structure. Higher-level quadratic configuration interaction calculations including single and double substitutions and energy contributions due to connected triples based on a restricted Hartree−Fock (HF) reference [RQCISD(T)], carried out by the same authors at the CASSCF(6,6)/6-31G* geometries, place the concerted transition structure 4.3 kcal mol^{-1} below the diradical intermediate. The RQCISD(T) activation energy of the concerted transition structure relative to reactants is 25.5 kcal mol^{-1}, which is a considerable improvement over the corresponding CASSCF-(6,6) figure of 43.8 kcal mol^{-1} and is very close to the experimental estimate of 25.1 ± 2 kcal mol^{-1}. This indicates that although the "6 in 6" CASSCF level of theory appears to provide an adequate description of the structural changes in the reacting system, the accurate prediction of the related energy barriers requires a higher-quality wave function. The CASSCF-(6,6) wave function takes into account the so-called "nondynamic" correlation effects within its "6 in 6" active space only, while the RQCISD(T) ansatz includes correlation effects (both "nondynamic" and "dynamic") for all electrons.

In a recent review, Borden and Davidson[22] emphasize the importance of including dynamic electron correlation effects in *ab initio* calculations and provide several examples of cases where wave functions which include only nondynamic correlation for the active electrons (such as CASSCF) may give results which are quantitatively and sometimes even qualitatively incorrect. Their examples include the differences between the CASSCF and RQCISD(T) energy barriers for the Diels−Alder reaction between *cis*-butadiene and ethene mentioned above, comparisons of the results of CASSCF calculations on the Cope rearrangement with those from two second-order perturbation theory treatments based on a CASSCF reference, CASPT2N[23] and CASMP2,[24] which account for (some of the) missing dynamic correlation, and results from CASSCF and higher-level calculations on excited states, radical cations and dehydrobenzenes. In the case of the Cope rearrangement, the inclusion of dynamic correlation effects leads to a significant change not only in the height of the activation barrier but also in the geometry of the transition structure.

Although the evidence adduced by Borden and Davidson is convincing, it is too early, in our opinion, to give up on "active space" methods: These methods introduce correlation just where chemical intuition suggests it is really necessary and thus significantly extend the range of systems that can be treated at a reasonable, beyond-HF level on current computational facilities. Unlike the HF approach, active space methods such as CASSCF and SC theory are capable of providing uniform-quality descriptions of the whole potential surface corresponding to a chemical process, including regions of bond-breaking and bond-formation. If chemical intuition is wrong in the initial choice of the active space, it is usually straightforward to modify this choice and enlarge the size of the active space until the quality of the wave function becomes acceptable. One example is provided by the SC description of the forbidden 2 + 2 cycloaddition of two ethene molecules,[25] where we found that our initial assumption of a four-orbital active space is insufficient for the description of the three C−C bonds and two "unpaired" electrons in the tetramethylene biradical intermediate at the same level of theory and we had to adopt an eight-orbital active space instead. In connection with this, it is also interesting to mention that early CASSCF(4,4)/4-31G calculations on the concerted transition structure of the Diels−Alder reaction between *cis*-butadiene and ethene[26,27] suggest noticeable alternation of C−C bond lengths: 1.389, 1.376, and 1.389 on the butadiene fragment and 1.398 on the ethene (all values in angstroms). On the other hand, recent larger CASSCF(6,6)/3-21G and CASSCF(6,6)/6-31G* results[20,21] indicate C−C bond equalization, consistent with the idea that the concerted transition structure is aromatic: 1.392 (1.398), 1.397 (1.397), and 1.392 (1.398) on the butadiene fragment and 1.400 (1.404) on the ethene moiety (all values in angstroms, 6-31G* results in parentheses).

Active space wave functions which already incorporate a significant amount of nondynamic correlation energy provide

(13) Sironi, M.; Cooper, D. L.; Raimondi, M.; Gerratt, J. *J. Chem. Soc., Chem. Commun.* **1989**, 675.
(14) Karadakov, P. B.; Gerratt, J.; Raos, G.; Cooper, D. L.; Raimondi, M. *Isr. J. Chem.* **1993**, *33*, 253.
(15) Karadakov, P. B.; Gerratt, J.; Cooper, D. L.; Raimondi, M.; Sironi, M. *Int. J. Quantum Chem.* **1996**, *60*, 545.
(16) Karadakov, P. B.; Ellis, M.; Gerratt, J.; Cooper, D. L.; Raimondi, M. *Int. J. Quantum Chem.* **1997**, *63*, 441.
(17) Wright, S. C.; Cooper, D. L.; Gerratt, J.; Raimondi, M. *J. Phys. Chem.* **1992**, *96*, 7943.
(18) Karadakov, P. B.; Gerratt, J.; Cooper, D. L.; Raimondi, M. *J. Phys. Chem.* **1995**, *99*, 10186.
(19) Borden, W. T.; Loncharich, R. J.; Houk, K. N. *Annu. Rev. Phys. Chem.* **1988**, *39*, 213.
(20) Li, Y.; Houk, K. N. *J. Am. Chem. Soc.* **1993**, *115*, 7478.
(21) Houk, K. N.; Li, Y.; Storer, J.; Raimondi, L.; Beno, B. *J. Chem. Soc., Faraday Symp.* **1994**, *90*, 1599.
(22) Borden, W. T.; Davidson, E. R. *Acc. Chem. Res.* **1996**, *29*, 67.
(23) Hrovat, D. A.; Morokuma, K.; Borden, W. T. *J. Am. Chem. Soc.* **1994**, *116*, 1072.
(24) Kozlowski, P. M.; Dupuis, M.; Davidson, E. R. *J. Am. Chem. Soc.* **1995**, *117*, 774.
(25) Karadakov, P. B.; Gerratt, J.; Cooper, D. L.; Raimondi, M. *J. Chem. Soc., Faraday Symp.* **1994**, *90*, 1643.
(26) Bernardi, F.; Botoni, A.; Robb, M. A.; Field, M. J.; Hillier, I. H.; Guest, M. F. *J. Chem. Soc., Chem. Commun.* **1985**, 1051.
(27) Bernardi, F.; Botoni, A.; Field, M. J.; Guest, M. F.; Hillier, I. H.; Robb, M. A.; Venturini, A. *J. Am. Chem. Soc.* **1988**, *110*, 3050.

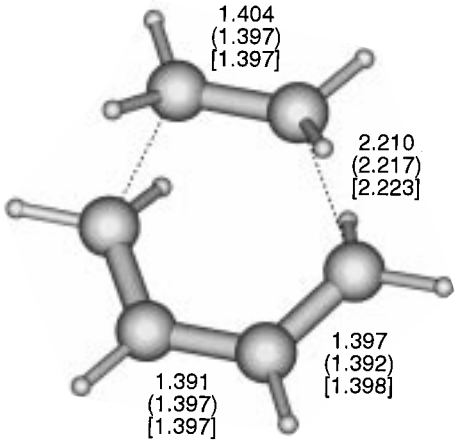

Figure 1. Carbon−carbon bond lengths (Å) at the TS of the Diels−Alder reaction. CASSCF(6,6)/4-31G values from the current work (top), followed by CASSCF(6,6)/3-21G (in parentheses) and CASSCF(6,6)/6-31G* (in brackets) values, taken from ref 21.

a much better reference for the construction of higher-level approaches than the standard HF ansatz. Borden and Davidson indicate[22] that, in order to match the results for the Cope rearrangement produced by second-order perturbation theory treatments constructed on top of a CASSCF reference (CASPT2N and CASMP2) by techniques based on a HF reference, one has to use either fourth-order Møller−Plesset perturbation theory with single, double, triple, and quadruple substitutions [MP4(SDQT)], or QCISD(T) or CCSD(T) (coupled-cluster approach including singles and doubles plus perturbative corrections for connected triple excitations). In cases where the closed-shell HF wave function is clearly inadequate, e.g., the dissociation of one of the O−H bonds in water,[28] HF-based constructions would have to include even higher excitations or orders of perturbation theory.

Our aim in this paper is not to reproduce the RQCISD(T) energy barriers for the gas-phase Diels−Alder reaction[20,21] through an alternative approach, but to show that the changes occurring during the course of this reaction inside the most compact wave function of near-CASSCF quality—the SC wave function—provide a clear and intuitive picture of the related bond-breaking and bond-formation processes, together with convincing evidence that the Diels−Alder transition structure is aromatic. It should be mentioned that the quantitative side of our results could be improved in a straightforward way by constructing small nonorthogonal CI (or "SC VB") expansions[29] on top of the SC wave functions along the reaction path. Past experience[29,30] indicates that while SC VB treatments of this type do provide more accurate numbers, as well as information about excited states, they do not change the qualitative nature of the model contained within the single-configuration SC reference wave function.

Computational Details

As a preliminary step, we located the concerted transition structure (TS) for the Diels−Alder reaction through a CASSCF(6,6)/4-31G calculation. Our TS geometry (C_s point group) is very similar to those obtained by Houk et al.[20,21] using CASSCF(6,6)/3-21G and CASSCF(6,6)/6-31G* wave functions (see Figure 1).

The most convenient and least biased way of tracing the changes in the geometry of the reacting system before and after the TS is to follow the minimum-energy path (MEP),[31,32] which is also known as the intrinsic reaction coordinate (IRC).[33,34] The MEP or IRC is defined as the union of steepest-descent paths, expressed in mass-weighted Cartesian coordinates, emerging from the saddle point corresponding to the TS and leading toward reactants and products. In the present paper, we employed the IRC algorithm of Gonzales and Schlegel[35,36] implemented in GAUSSIAN94,[1] which was the package used for all non-SC computational work.

Just as in the case of the TS, the IRC calculations were performed at the CASSCF(6,6)/4-31G level of theory and involved six points in the TS → product direction and another six points in the TS → reactants direction, in steps of 0.1 amu$^{1/2}$ bohr along the path. The determination of the CASSCF wave functions at the start of the TS geometry optimization and at the first point of the IRC was preceded, as usual, by standard HF calculations, providing initial guesses for the orbitals. Additionally, we performed separate HF calculations at each of the remaining 12 IRC points.

The SC counterpart to the 6 in 6 CASSCF wave function for the Diels−Alder cycloaddition also involves six active orbitals $\psi_1-\psi_6$:

$$\Psi^6_{00} = \hat{A}\,[(\prod_{i=1}^{20}\varphi_i\alpha\varphi_i\beta)(\prod_{\mu=1}^{6}\psi_\mu)\Theta^6_{00}] \qquad (1)$$

These active orbitals are all singly occupied and nonorthogonal, and we shall refer to them as valence or spin-coupled orbitals. φ_i stand for the doubly occupied inactive orbitals holding the core electrons and Θ^6_{00} denotes the active space spin function—a general linear combination of all five unique spin-coupling schemes for a singlet system of six electrons:

$$\Theta^6_{00} = \sum_{k=1}^{5} C_{0k}\Theta^6_{00;k} \qquad (2)$$

(the pairs of zero subscripts in Ψ^6_{00}, Θ^6_{00}, and $\Theta^6_{00;k}$ indicate the values of the total spin S and its z projection M, $S = M = 0$).

The active and core orbitals are approximated, just as in molecular orbital theory, by linear expansions in a suitable basis of atomic orbitals (AOs) contributed by all atoms in the system. Their form is determined through simultaneous optimization of the energy expectation value corresponding to wave function (1) with respect to the AO expansion coefficients for the core and active orbitals and the spin-coupling coefficients C_{0k} [see eq 2]. Almost all of the fully variational SC calculations in the present paper were performed with a very efficient new code (CASVB)[37,38] which exploits the invariance of CAS wave functions to nonsingular transformations of the active orbitals and which is available within MOLPRO.[39] Calculations with the older code described in ref 40 were performed only at the TS and at both ends of the IRC segment which we studied, mainly for comparisons and to assist orbital plotting. The basis set employed in all the SC computational work was 4-31G, identical to that used in the preliminary HF and CASSCF calculations.

(28) Handy, N. C.; Knowles, P. J.; Somasundran, K. *Theor. Chim. Acta* **1985**, *68*, 87.
(29) Gerratt, J.; Raimondi, M. *Proc. R. Soc. London, Ser. A* **1980**, *371*, 525.
(30) Da Silva, E. C.; Gerratt, J.; Cooper, D. L.; Raimondi, M. *J. Chem. Phys.* **1994**, *101*, 3866.
(31) Truhlar, D. G.; Kuppermann, A. *J. Am. Chem. Soc.* **1971**, *93*, 1840.
(32) Truhlar, D. G.; Kuppermann, A. *J. Chem. Phys.* **1972**, *56*, 2232.
(33) Fukui, K. *J. Chem. Phys.* **1970**, *74*, 4161.
(34) Fukui, K. In *The World of Quantum Chemistry. Proceedings of the First International Congress of Quantum Chemistry, Menton, 1973*; Daudel, R., Pullman, B., Eds.; D. Reidel: Dordrecht, The Netherlands, 1974; p 113.
(35) Gonzalez, C.; Schlegel, H. B. *J. Chem. Phys.* **1989**, *90*, 2154.
(36) Gonzalez, C.; Schlegel, H. B. *J. Phys. Chem.* **1990**, *94*, 5523.
(37) Thorsteinsson, T.; Cooper, D. L.; Gerratt, J.; Karadakov, P. B.; Raimondi, M. *Theor. Chim. Acta* **1996**, *93*, 343.
(38) Thorsteinsson, T.; Cooper, D. L. *Theor. Chim. Acta* **1996**, *94*, 233.
(39) Werner, H.-J.; Knowles, P. J., with contributions from Amos, R. D.; Berning, A.; Cooper, D. L.; Deegan, M. J. O.; Dobbyn, A. J.; Eckert, F.; Hampel, C.; Leininger, T.; Lindh, R.; Lloyd, A. W.; Meyer, W.; Mura, M. E.; Nickla, A.; Palmieri, P.; Peterson, K.; Pitzer, R.; Pulay, P.; Rauhut, G.; Schütz, M.; Stoll, H.; Stone, A. J.; Thorsteinsson, T. *MOLPRO (A Package of Ab Initio Programs)*.
(40) Karadakov, P. B.; Gerratt, J.; Cooper, D. L.; Raimondi, M. *J. Chem. Phys.* **1992**, *97*, 7637.

For the purposes of the present investigation it is most convenient to construct the full spin space using the Rumer basis.[41] Each of the spin eigenfunctions $\Theta^6_{00;1} - \Theta^6_{00;5}$ represents a product of three singlet two-electron spin functions:

$$\Theta^6_{00;1} = (\alpha\beta)(\alpha\beta)(\alpha\beta) \equiv (1{-}2, 3{-}4, 5{-}6)$$

$$\Theta^6_{00;2} = (\alpha(\alpha\beta)\beta)(\alpha\beta) \equiv (1{-}4, 2{-}3, 5{-}6)$$

$$\Theta^6_{00;3} = (\alpha\beta)(\alpha(\alpha\beta)\beta) \equiv (1{-}2, 3{-}6, 4{-}5)$$

$$\Theta^6_{00;4} = (\alpha(\alpha\beta)(\alpha\beta)\beta) \equiv (1{-}6, 2{-}3, 4{-}5)$$

$$\Theta^6_{00;5} = (\alpha(\alpha(\alpha\beta)\beta)\beta) \equiv (1{-}6, 2{-}5, 3{-}4) \quad (3)$$

The two notations used in these definitions can be explained as follows: In the first one, a singlet pair is associated with each combination of an α and a β spin function enclosed within a matching pair of left and right parentheses; for example, in $(\alpha(\alpha\beta)(\alpha\beta)\beta)$ the pairs couple the spins of the electrons in the first and sixth, second and third, and fourth and fifth SC orbitals, respectively. In the second notation, all electron pairs are indicated explicitly. The graphical representation of Rumer spin functions involves Rumer diagrams which closely resemble the resonance structures that populate the pages of older organic chemistry textbooks. There is a one-to-one correspondence between $\Theta^6_{00;1} - \Theta^6_{00;5}$ and the well-known five resonance structures for benzene: $\Theta^6_{00;1} \leftrightarrow K_1$, $\Theta^6_{00;2} \leftrightarrow D_1$, $\Theta^6_{00;3} \leftrightarrow D_2$, $\Theta^6_{00;4} \leftrightarrow K_2$ and $\Theta^6_{00;5} \leftrightarrow D_3$ where K_1 and K_2 and D_1, D_2, and D_3 are the two Kekulé and three Dewar structures, respectively.

In addition to Rumer spin eigenfunctions, SC calculations often make use of two other spin bases introduced by Kotani and Serber (for details, see ref 41). The interconversion between active space spin functions (such as Θ^6_{00} in eq 2) expressed in the Rumer, Kotani, and Serber spin bases has become a trivial task with the introduction of a specialized code for the symbolic generation and transformation of spin eigenfunctions (SPINS; see ref 42). We have also recently exploited certain computational advantages associated with character-projected spin functions.[43,44]

For evaluating the relative weights of the individual Rumer spin functions (3) as components of the overall spin function for the active electrons (2), use can be made of one of the following two expressions, due to Chirgwin and Coulson[45] and Gallup and Norbeck,[46] respectively:

$$P^{CC}_{0k} = C_{0k}\sum_{l=1}^{5}(\langle\mathbf{\Theta}^6_{00}|\mathbf{\Theta}^6_{00}\rangle)_{kl}C_{0l} \quad \text{(it is assumed that } \langle\Theta^6_{00}|\Theta^6_{00}\rangle = 1) \quad (4)$$

$$P^{GN}_{0k} = c(C_{0k})^2/(\langle\mathbf{\Theta}^6_{00}|\mathbf{\Theta}^6_{00}\rangle^{-1})_{kk} \quad c^{-1} = \sum_{k=1}^{5}(C_{0k})^2/(\langle\mathbf{\Theta}^6_{00}|\mathbf{\Theta}^6_{00}\rangle^{-1})_{kk} \quad (5)$$

where $\langle\mathbf{\Theta}^6_{00}|\mathbf{\Theta}^6_{00}\rangle$ denotes the 5×5 overlap matrix between spin functions (3). One advantage of the Gallup−Norbeck expression over the older Chirgwin−Coulson formula is that P^{GN}_{0k} are nonnegative by construction, while in some cases P^{CC}_{0k} can attain nonphysical negative values. The link between the SC approach and classical VB theory is revealed by an alternative representation of the SC wave function (1) as a sum of five VB-style "structures"

$$\Psi^6_{00} = C_{01}\Psi_{K_1} + C_{02}\Psi_{D_1} + C_{03}\Psi_{D_2} + C_{04}\Psi_{K_2} + C_{05}\Psi_{D_3} \quad (6)$$

where

$$\Psi_{K_1} = \hat{A}\,[(\text{core})(\text{valence})\Theta^6_{00;1}] \quad \Psi_{D_1} = \hat{A}\,[(\text{core})(\text{valence})\Theta^6_{00;2}]$$

$$\Psi_{D_2} = \hat{A}\,[(\text{core})(\text{valence})\Theta^6_{00;3}] \quad \Psi_{K_2} = \hat{A}\,[(\text{core})(\text{valence})\Theta^6_{00;4}]$$

$$\Psi_{D_3} = \hat{A}\,[(\text{core})(\text{valence})\Theta^6_{00;5}]$$

The VB "resonance" energy for any structure is then given by the difference between its energy expectation value and the full SC energy. As a rule, the VB resonance energy for a molecule corresponds to that for the dominant structure, i.e., for the structure with the largest P^{CC}_{0k} or P^{GN}_{0k} (see eqs 4 an 5). In the case of benzene, for example, the VB resonance energy is given by $E(\Psi_{K_1}) - E(\Psi^6_{00})$.[12] Despite the similar terminology,VB resonance energies should not be compared to experimental resonance (or delocalization) energies calculated on the basis of the enthalpies of hydrogenation reactions which are different quantities and require another computational approach for their theoretical evaluation (see, e.g., ref 47).

Results and Discussion

The energy profiles along the CASSCF(6,6) IRC at the HF, SC, and CASSCF(6,6) levels are shown in Figure 2. The SC and CASSCF(6,6) curves are much lower than the HF one and very close together. The amount of CASSCF(6,6) correlation energy recovered by the SC wave function is rather uniform, being 95.4% and 95.8% at the "−" and "+" ends of the IRC segment and 92.9% at the TS, respectively. This justifies the use of SC theory to study the evolution of the electronic structure of the reacting system at geometries coming from a preliminary CASSCF IRC calculation. The percentage of CASSCF(6,6) correlation energy contained within the SC wave function describing the TS of the Diels−Alder reaction is slightly higher than the corresponding figure for benzene: 89.6% using a TZVP basis.[12]

On its own, the fact that the whole active space of the SC wave function (1) undergoes substantial changes during the course of the cycloaddition process is hardly unexpected. The surprise comes with the way in which the individual changes in the shapes of the active orbitals $\psi_1-\psi_6$ and in the values of the spin-coupling coefficients $C_{01}-C_{05}$ piece together to provide a lucid picture of the electronic mechanism of the Diels−Alder reaction.

Figure 3 shows snapshots of the shapes of the symmetry-unique SC orbitals as three-dimensional isovalue surfaces taken at the two ends of the IRC segment which we investigated and at the TS. The remaining orbitals can be obtained easily from those in the figure through reflections in the σ_h plane passing through the middles of the ethene and central butadiene C−C bonds: $\sigma_h\psi_1 = \psi_4$, $\sigma_h\psi_2 = \psi_3$, and $\sigma_h\psi_6 = \psi_5$.

At IRC = 0.6 amu$^{1/2}$ bohr the butadiene and ethene fragments are still well-separated. Orbitals ψ_1 and ψ_2 clearly form one of the two butadiene π bonds, while the second one is formed by ψ_3 and ψ_4 (not shown). As one would expect, ψ_2 has a small additional bulge toward ψ_3 which is a consequence of the weaker π orbital interaction across the central carbon−carbon bond. Orbital ψ_6 and its symmetry-related counterpart ψ_5 describe the π bond on the ethene fragment. It should be mentioned that although the shapes of the SC orbitals are very similar to those for typical conjugated systems (see, e.g., ref

(41) Pauncz, R. *Spin Eigenfunctions*; Plenum Press: New York, 1979.
(42) Karadakov, P. B.; Gerratt, J.; Cooper, D. L.; Raimondi, M. *Theor. Chim. Acta* **1995**, *90*, 51.
(43) Friis-Jensen, B.; Cooper, D. L.; Rettrup, S. *Theor. Chim. Acta* **1998**, *99*, 8.
(44) Friis-Jensen, B.; Cooper, D. L.; Rettrup, S. *J. Math. Chem.* **1997**, *22*, 249.
(45) Chirgwin, B. H.; Coulson, C. A. *Proc. R. Soc. London, Ser. A* **1950**, *201*, 196.
(46) Gallup, G. A.; Norbeck, J. M. *Chem. Phys. Lett.* **1973**, *21*, 495.
(47) Foresman, J. B.; Frisch, Æ. *Exploring Chemistry with Electronic Structure Methods*; Gaussian, Inc.: Pittsburgh, PA, 1996.

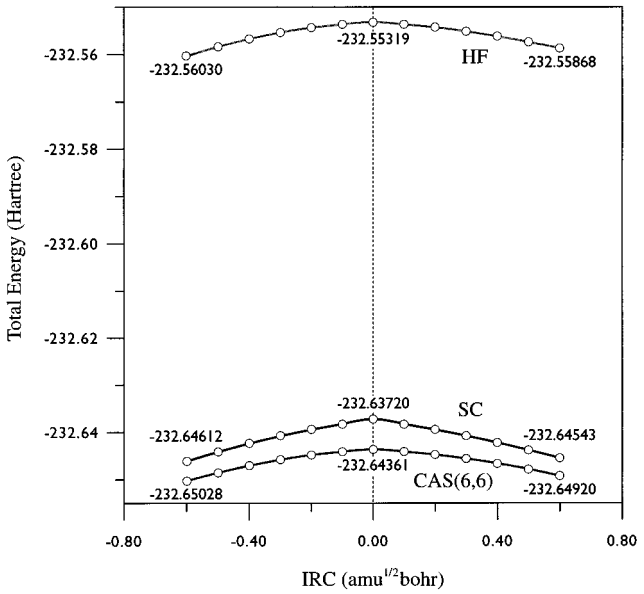

Figure 2. HF, SC, and CASSCF(6,6) energy profiles for the Diels−Alder reaction along the CASSCF(6,6) IRC. The energies at IRC = −0.6 amu$^{1/2}$ bohr, TS (IRC = 0), and IRC = 0.6 amu$^{1/2}$ bohr are indicated explicitly below and above the corresponding curves.

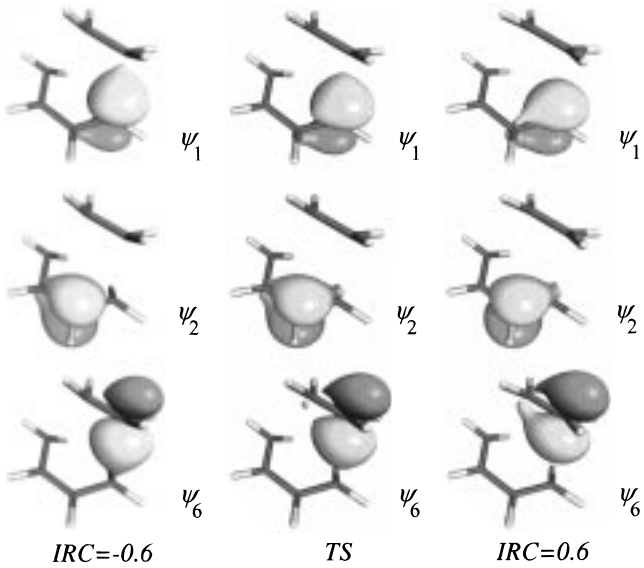

Figure 3. Valence orbitals ψ_1, ψ_2, and ψ_6 from the SC wave function for the Diels−Alder reaction at IRC = −0.6 amu$^{1/2}$ bohr, TS (IRC = 0), and IRC = 0.6 amu$^{1/2}$ bohr. Three-dimensional isovalue surfaces corresponding to $\psi_\mu \pm 0.08$, drawn from virtual reality modeling language (VRML) files produced by MOLDEN.[51]

48), at this point on the IRC curve the tetrahedralization of the ethene and terminal butadiene carbons has already started but it is still insufficiently advanced to induce considerable changes in the appearance of the orbitals.

At the TS (IRC = 0 amu$^{1/2}$ bohr) the shapes of the SC orbitals are already noticeably different from those on the separated fragments. The tail of ψ_1 in the direction of ψ_2 disappears almost entirely; while at IRC = 0.6 amu$^{1/2}$ bohr this orbital resembles a distorted carbon $2p_\pi$ AO, at the TS it looks as though it is halfway through a mutation to a distorted sp^3 hybrid. This fact, together with the parallel change in the shape of ψ_6, indicates that the bonds in which ψ_1 and ψ_6 used to participate well before the TS, between ψ_1 and ψ_2, and ψ_5 and ψ_6,

(48) Karadakov, P. B.; Gerratt, J.; Cooper, D. L.; Raimondi, M. *J. Am. Chem. Soc.* **1993**, *115*, 6863.

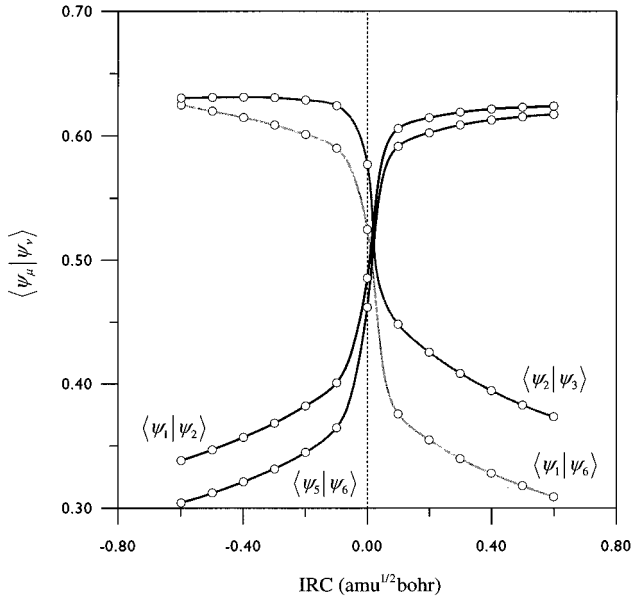

Figure 4. Variation of the overlap integrals $\langle\psi_\mu|\psi_\nu$ between neighboring SC orbitals along the CASSCF(6,6) IRC for the Diels−Alder reaction.

Table 1. Overlaps between Neighboring Orbitals from the SC Wave Functions for the Diels−Alder Cycloaddition Reaction at IRC = −0.6 amu$^{1/2}$ bohr, TS (IRC = 0), and IRC = 0.6 amu$^{1/2}$ bohr

quantity	IRC = −0.6	TS	IRC = 0.6
$\langle\psi_1\|\psi_2\rangle$	0.338	0.485	0.624
$\langle\psi_2\|\psi_3\rangle$	0.630	0.577	0.373
$\langle\psi_5\|\psi_6\rangle$	0.304	0.462	0.617
$\langle\psi_1\|\psi_6\rangle$	0.625	0.525	0.309

respectively, are now being broken simultaneously with the formation of a new bond between ψ_1 and ψ_6. An identical process takes place at the other end of the butadiene fragment: A marked decrease in the bonding interaction between orbitals ψ_3 and ψ_4 and a re-engagement of ψ_4 in a new bond with ψ_5. The remaining two orbitals, ψ_2 and ψ_3, of which we have shown only the first, are the most interesting as they closely resemble in form the SC orbitals for benzene[10−12] and appear to be almost equally distorted toward one another (these distortions will eventually lead to the formation of the cyclohexene π bond) and toward their former partners in the butadiene π bonds, ψ_1 and ψ_4, respectively.

The new bonding interactions which were just a little more than hints within the TS orbitals are much more noticeable at IRC = − 0.6 amu$^{1/2}$ bohr. The shapes of ψ_1 and ψ_6 are now quite similar and much more sp^3-like, while ψ_2 is clearly engaged together with ψ_3 in a new π bond.

The changes in the shapes of the SC orbitals with the progress of the cycloaddition process are paralleled by the behavior of the overlap integrals $\langle\psi_\mu|\psi_\nu\rangle$ (see Figure 4). We show only the curves corresponding to overlaps between neighboring orbitals, i.e., orbitals which are involved in actual bonding interactions at some stage of the cycloaddition process. The numerical values of these overlaps at the TS and at IRC = ±0.6 amu$^{1/2}$ bohr are presented in Table 1. As the reactants approach each other, the overlaps $\langle\psi_1|\psi_2\rangle = \langle\psi_3|\psi_4\rangle$ and $\langle\psi_5|\psi_6\rangle$ corresponding to the π bonds on the butadiene and ethene fragments, respectively, begin to decrease. At the same time, the overlap $\langle\psi_2|\psi_3\rangle$ between the SC orbitals on the two central butadiene carbons and the overlaps $\langle\psi_1|\psi_6\rangle = \langle\psi_4|\psi_5\rangle$ between opposite orbitals on the two reactants are on the increase. As the overlap curves pass through the TS, they undergo very rapid

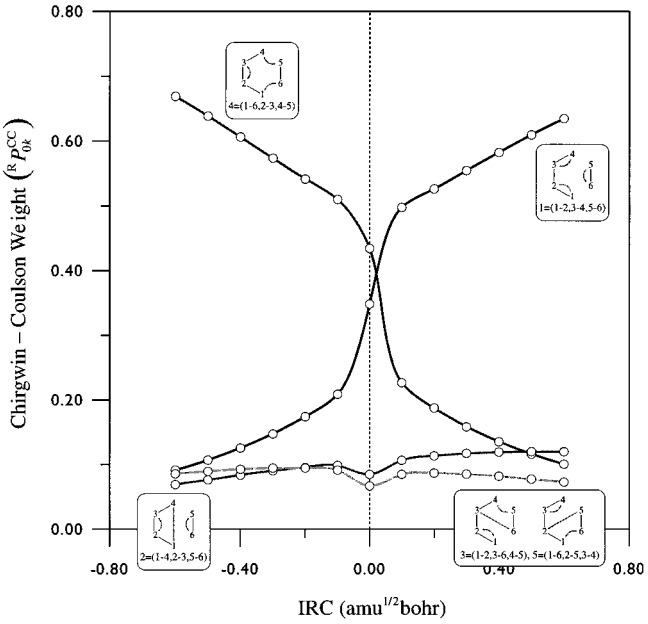

Figure 5. Composition of the active space spin-coupling pattern Θ_{00}^{6} (see eq 2) from the SC wave function for the Diels−Alder reaction along the CASSCF(6,6) IRC, expressed in terms of Chirgwin−Coulson weights.

changes. These occur within a short IRC interval, no longer than 0.2 amu$^{1/2}$ bohr. An important feature of the overlap curves is that they come very near to crossing in a single point just before the TS on the side of the reactants. At this point all overlaps between neighboring orbitals become almost equal. The common value that can be deduced from the plots is approximately 0.51, which is remarkably close to the overlap between neighboring orbitals in benzene (0.52; see ref 12). After the TS, in the direction of the product, the largest overlaps become those that correspond to the newly formed bonds, $\langle\psi_1|\psi_6\rangle = \langle\psi_4|\psi_5\rangle$ and $\langle\psi_2|\psi_3\rangle$, while those related to breaking bonds, $\langle\psi_1|\psi_2\rangle = \langle\psi_3|\psi_4\rangle$ and $\langle\psi_5|\psi_6\rangle$, decrease rapidly. It is interesting to observe that after the TS the overlap $\langle\psi_2|\psi_3\rangle$ initially increases faster than $\langle\psi_1|\psi_6\rangle = \langle\psi_4|\psi_5\rangle$, but then quickly reaches a plateau at which its value (approximately 0.64) is in very good agreement with that for a typical π bond (0.629 for ethene; see ref 48). This suggests that the hexadiene π bond is established at a slightly earlier stage of the reaction in comparison to the σ bonds which close the cycle.

The changes in the orbital shapes and overlaps illustrate just one of the two most important aspects of the SC representation of the processes of bond-breaking and bond formation. The second important aspect is related to the fact that during processes of this type the way in which the spins of the SC orbitals are coupled together usually undergoes significant changes, as required to accommodate the differences in the electronic structures of reactants and products. The variations in the composition of the active space spin function Θ_{00}^{6} (see eq 2) over the segment of the IRC for the Diels−Alder reaction which we investigated are shown in Figure 5 (see also Table 2). As the Gallup−Norbeck weights P_{0k}^{GN} (see eq 5) behave very similarly to the Chirgwin−Coulson weights P_{0k}^{CC} (see eq 4), we do not show the corresponding plots.

At each of the two ends of the IRC segment the spin function is dominated by just one of its five components. At IRC = 0.6 amu$^{1/2}$ bohr the main spin-coupling pattern is the first Kekulé-type Rumer spin eigenfunction (1−2, 3−4, 5−6), while the second Kekulé-type Rumer spin eigenfunction (1−6, 2−3, 4−5) prevails at the other end of the IRC segment, IRC = −0.6 amu$^{1/2}$ bohr. This is consistent, respectively, with the bonding in the reacting butadiene and ethene molecules and in the result of their cycloaddition: cyclohexene. Similarly to the plots of the SC orbital overlaps (see Figure 4), the most interesting region is in the close vicinity of the TS where, within an IRC interval of approximately 0.2 amu$^{1/2}$ bohr, the active space spin function switches from a form appropriate for the reactants to a form more suited to the product. The crossing point of the P_{01}^{CC} and P_{04}^{CC} curves is at an IRC value which is visually indiscernible from the approximate crossing point of the overlap curves in Figure 4.

Table 2. Chirgwin−Coulson ($^{R}P_{0k}^{CC}$) and Gallup−Norbeck ($^{R}P_{0k}^{GN}$) Weights Defining the Compositions of the Active Space Spin Functions for the Diels−Alder Reaction in the Rumer Spin Basis at IRC = −0.6 amu$^{1/2}$ bohr, TS (IRC = 0), and IRC = 0.6 amu$^{1/2}$ bohr

	IRC = −0.6		TS		IRC = 0.6	
k	$^{R}P_{0k}^{CC}$	$^{R}P_{0k}^{GN}$	$^{R}P_{0k}^{CC}$	$^{R}P_{0k}^{GN}$	$^{R}P_{0k}^{CC}$	$^{R}P_{0k}^{GN}$
1	0.091 31	0.048 32	0.347 76	0.387 24	0.634 61	0.805 72
2	0.068 76	0.027 60	0.084 72	0.038 78	0.119 66	0.074 36
3	0.085 50	0.040 36	0.066 71	0.025 39	0.072 62	0.031 66
4	0.668 93	0.843 36	0.434 08	0.523 20	0.100 48	0.056 59
5	0.085 50	0.040 36	0.066 71	0.025 39	0.072 62	0.031 66

The analysis of Figures 4 and 5 indicates that during the Diels−Alder cycloaddition the reacting system passes through a very short interval of IRC values (it is tempting to say "through a point", but we are not allowed to do so because of the interpolated nature of all curves) situated immediately before the TS on the side of the reactants, throughout which its electronic structure closely reminds us of that of benzene. Not only do some of the TS orbitals [ψ_2 (see Figure 2) and its symmetry-related counterpart ψ_3] strongly resemble the SC orbitals for benzene, but also the overlaps between neighboring SC orbitals all attain a virtually identical value, almost equal to that for benzene, and the weights of the two Kekulé-type Rumer spin-coupling schemes become identical, indicating a well-known resonance usually associated with benzene. Although these facts should be sufficiently convincing on their own, we decided to seek further support for the aromaticity of the TS for the Diels−Alder reaction by calculating the VB resonance energies corresponding to structures K_1 and K_2 (see eq 6): $E(\Psi_{K_1}) - E(\Psi_{00}^{6}) = 106$ kJ mol^{-1} and $E(\Psi_{K_2}) - E(\Psi_{00}^{6}) = 66$ kJ mol^{-1}. Clearly, the difference between these two resonance energies would be smaller if they were calculated at the crossing point of the curves in Figures 4 and 5, but even at the TS the numbers are reasonably close to the resonance energy for benzene (88 kJ mol^{-1}, DH basis, see ref 12).

The changes in the shapes of the SC orbitals and in the nature of the spin-coupling pattern along the reaction path strongly suggest that the two π bonds on the butadiene fragment and the ethene π bond break simultaneously, and that the formation of the two new σ bonds that close the cyclohexene ring and of the cyclohexene π bond also takes place almost in parallel. During the whole process each SC orbital remains distinctly associated with a single carbon atom while its form adjusts to accommodate the differences in the nature of bonding between reactants and product. If we want to express all of this using arrows or half-arrows, as is usually done in organic chemistry textbooks, it would be most appropriate to use half-arrows as in **A** below. Having in mind the SC description of the Diels−Alder cycloaddition, we may say that the significance of the half-arrows is two-fold: they indicate (i) the simultaneous processes of bond-breaking and bond formation, during which

the orbitals change in shape, but remain on the same carbon and (ii) the recoupling of spins during which the initial singlet pairs associated with the butadiene and ethene π bonds [see the curve for (1−2, 3−4, 5−6) in Figure 5] are replaced by singlet pairs coupling the orbitals participating in the new σ bonds and in the cyclohexene π bond [see the curve for (1−6, 2−3, 4−5) in Figure 5].

A illustrates the "homolytic" mechanism for the Diels−Alder reaction, while **B** corresponds to the "heterolytic" mechanism.[49] In this case the terms homolytic and heterolytic are devoid of their usual meanings, which is a consequence of the fact that the reacting system does not pass through a biradical or a zwitterionic intermediate. In many recent organic chemistry textbooks one can find a picture of **B** only, accompanied by a safeguarding remark that the scheme is not meant to illustrate the real reaction mechanism (which does make one wonder why it should be there in the first place). The results from this paper indicate that **B** is, in fact, misleading and if one needs to use a simplistic representation of the mechanism of the Diels−Alder cycloaddition, **A** would be much more appropriate.

Conclusions

The work presented in this paper constitutes one of the first attempts to obtain a qualitative description of the electronic mechanism of a pericyclic reaction based on a post-HF wave function. It also introduces a novel use of the IRC approach which until now has been employed mainly in order to prove that a given TS connects the minima corresponding to reactants and products in a chemical reaction.

The SC wave function incorporates, by definition, all the components necessary for a proper qualitative description of any changes in the electronic structure of the reacting system which might take place during a cycloaddition process. As we have shown here for the example of the gas-phase Diels−Alder reaction, all of these components are, indeed, put to a very good use. The evolution of the shapes of the six SC orbitals along the reaction path provides a visual illustration of the breaking of existing bonds and formation of new ones that take place in parallel as the system proceeds from reactants to product. The fact that the SC orbitals are nonorthogonal eliminates possible spurious nodal surfaces; the related nonzero overlap values furnish numerical estimates of the progress of the ongoing bond reformation processes. Finally, the changes in the way in which the spins of the six SC orbitals are coupled together to an overall singlet show how the dominant Kekulé-type Rumer spin function involving the π electron pairs in butadiene and ethene gradually gives way to the second Kekulé-type Rumer spin function which incorporates the electron pairs from the two new σ bonds and the cyclohexene π bond. We have shown that over a very short IRC interval near the TS these two Kekulé spin functions have almost identical weights which, together with other similarities in orbital shapes, orbital overlaps, and VB resonance energy values, allows us to claim that the electronic structure of the TS of the Diels−Alder reaction strongly resembles that of benzene. This is convincing evidence for its aromaticity.

The aromaticity of the transition structures for different pericyclic reactions has been analyzed using different criteria: energies of concert, C−C bond equalization, ring-current effects (see, e.g., ref 50 and references therein). As we have shown for the example of the Diels−Alder cycloaddition, the SC approach allows a more straightforward and intuitive alternative criterion which is based on the direct comparison of the SC wave function for the TS with that for benzene and does not require the calculation of any additional properties.

The changes within the SC wave function during the Diels−Alder cycloaddition are consistent with a homolytic mechanism, in which all SC orbitals participating in the bonds being reformed remain permanently attached to the same carbon atom throughout the reaction. Information of this type cannot be provided by the HF wave function because of the double occupancy of all orbitals; although it is embedded inside the CASSCF wave function, to obtain it, one would need to perform a transformation of the CASSCF wave function to a VB-style (in fact, SC-style!) representation.[37]

Our choice of the CASSCF approach for studying the changes in the geometry of the reacting system was determined by the availability of an efficient geometry optimizer and IRC routines inside GAUSSIAN94.[1] However, the fact that codes capable of doing SC calculations are now being incorporated into large general-purpose *ab initio* codes such as MOLPRO[39] suggests that soon it will be possible to do all calculations necessary for establishment of an intuitive, easy-to-visualize theoretical model of a reaction mechanism at the SC level.

One important conclusion following from our analysis of the mechanism of the Diels−Alder reaction is that the changes in the electronic structure of the reacting system are much more sudden than the changes in its geometry. All major alterations in the SC wave function take place within a short IRC interval of about 0.2 amu$^{1/2}$ bohr, throughout which the geometry of the system does not change very significantly. For this reason, if an attempt had been made to look at the changes of the delocalized orbitals inside the standard HF or CASSCF wave function along the same interval, it would not have been possible to discern any major differences and to derive an electronic reaction mechanism.

This promising debut of the combination between the SC approach and IRC calculations shows that modern VB theory is capable of substantiating or refuting the half- and full-arrow electronic mechanisms, so popular with organic chemists, by comparing them to clear-cut changes in orbital shapes and resonance patterns, stemming from near-CASSCF-quality wave functions.

JA9741741

(49) Reutov, O. A. *Fundamentals of Theoretical Organic Chemistry*; North-Holland: New York, 1967.

(50) Jiao, H.; Schleyer, P. v. R. *J. Chem. Soc., Faraday Symp.* **1994**, *90*, 1559.

(51) Schaftenaar, G. *MOLDEN (A Pre- and Postprocessing Program of Molecular and Electronic Structure)*; CAOS/CAMM Center: University of Nijmegen, The Netherlands.